

PAPER • OPEN ACCESS

## Ignition and burning characterization of edible oils

To cite this article: Alain Alonso *et al* 2024 *J. Phys.: Conf. Ser.* **2885** 012025

View the [article online](#) for updates and enhancements.

You may also like

- [Simulation and Performance of  \$^{99}\text{Mo}/^{99\text{m}}\text{Tc}\$  Radioisotope Separation by Modified Extraction Method](#)  
P. Chaidir, F. Yoshitaka, S. Indra et al.
- [Workshop on Young Crescent Moon: Visibility Limit and Digital Image Contrast](#)  
M. Hasan Faadillah, Martha Kurniasari, Cahyo P. Asmoro et al.
- [Using Large Language Models to Recommend Repair Actions for Offshore Wind Maintenance](#)  
C Walker, C Rothon, K Aslansefat et al.



**UNITED THROUGH SCIENCE & TECHNOLOGY**

 **The Electrochemical Society**  
Advancing solid state & electrochemical science & technology

**248th  
ECS Meeting**  
Chicago, IL  
October 12-16, 2025  
*Hilton Chicago*

**Science +  
Technology +  
YOU!**

**SUBMIT  
ABSTRACTS by  
March 28, 2025**

**SUBMIT NOW**

# Ignition and burning characterization of edible oils

Alain Alonso<sup>1</sup>, Mariano Lázaro<sup>1</sup>, Cristina Rueda<sup>2</sup>, Emilio Placer<sup>2</sup>, Daniel Alvear<sup>1</sup>

<sup>1</sup>GIDAI group, Universidad de Cantabria, Avda. Los Castros, s/n, Santander. Spain

<sup>2</sup>BSH Electrodomésticos España S.A., Centro de Desarrollo de Gas, C. Eduardo García, 30, Santander. Spain

alonsoia@unican.es

**Abstract.** Regardless of the country or geographical area, kitchens are the rooms where fires are most likely to begin in homes, and cooking is the leading cause. Statistics consistently demonstrate that cooking fires primarily occur due to the ignition of cooking materials. Consequently, understanding the thermal properties and combustion behaviour of edible oils is crucial for developing effective fire prevention, detection and suppression strategies. In this work, three oils (soybean, rapeseed, and sunflower) are analysed, namely, their behaviour at high temperatures by identifying parameters such as the time to ignition, critical heat flux, thermal response parameter, and effective heat of combustion. The results obtained showed that edible oils required a high temperature to reach ignition, however, once reached the energy released was similar to other liquid fuels employed for combustion purposes.

## 1. Introduction

Statistics indicate that kitchen fires are a widespread and potentially life-threatening hazard, accounting for a substantial portion of residential fires globally. Cooking is the leading cause of residential fires, accounting for approximately 50% of all fires [1]. Unattended cooking, resulting in the overheating of oils and fats to their ignition point, is the leading cause of these fires, accounting for 31% [2].

Understanding the thermal properties of cooking materials, especially edible oils, is crucial for comprehending their behaviour during heating and combustion phases, for reducing the fire risk in domestic housing. Previous full-scale analyses of kitchen fires [3,4], characterizing the energy released from cooking oil ignition, provided valuable insights into enclosure effects and contribution to fire development from on surrounding items within a cooking area. Nonetheless, these studies present challenges in characterizing the ignition conditions of the combustible (e.g., ignition time, critical heat flux, burning rate). To address this, calorimetric cone tests have been employed for the thermal characterization of various edible oils, vegetable oil residues and fats collected from extractor hoods.

This study aims to understand the ignition of commonly used cooking oils and their burning rates. The ignition process for condensed fuels involves three key stages: gasification (pyrolysis) of the fuel, mixing of the fuel vapour with an oxidizer (typically air), and subsequent ignition of the mixture. Each stage requires a specific time scale. By comparing the typical times for the gasification, mixing, and chemistry process, it is clear that the gasification time for a liquid fuel is much greater than the mixing and chemistry times. Therefore, this work defines the gasification time as the fuel ignition time. Therefore, gasification time is defined as fuel ignition time in this work. The hazard of liquid fuels is well-established to be linked to their vapour pressure and subsequent flammable limits. This relationship is reflected in the flash point, which is the minimum temperature at which a liquid produces enough



vapour to ignite when exposed to a spark or flame [5]. While the flash point apparatus is designed specifically to determine this property, it does not provide valuable information on other fire behaviour characteristics, such as Mass Loss Rate (MLR), Heat Release Rate (HRR) and Critical Heat Flux (CHF). Bench-scale cone calorimetry offers valuable insights into the flammability of these oils when exposed to elevated temperatures, providing crucial data to explain three key characteristics of fires involving cooking oils: i) these fires can readily escalate into larger events, ii) extinguishing such fires requires a relatively challenging task, and iii) the risk of re-ignition is significantly increased if the oil is not properly cooled after extinguishing.

The ignition is strongly correlated with the external heat flux applied ( $\dot{q}_{ext}''$ ) over a specific time period, known as the time to ignition (TTI)( $t_{ign}$ ) [6], and they are related with Equation 1:

$$\dot{q}_{0,ing}'' = h_t (T_{ign} - T_{\infty}) \quad (1)$$

Where the ( $\dot{q}_{0,ing}''$ ) is the critical heat flux (CHF),  $h_t$  is the total heat transfer coefficient and  $T_{ign}$  and  $T_{\infty}$  are the auto ignition and ambient temperature respectively.

The first two key parameters analysed are the TTI and CHF. Consequently, if a sample is exposed to a specific heat flux for a duration less than the TTI, or if the applied heat flux does not reach the CHF value, the sample will not ignite regardless of the total exposure time to the external heat flux. The CHF is determined experimentally by observing the time to ignition at various external heat fluxes. For thermally thin samples ( $Biot < 0,1$ ), the inverse of the ignition time, and for thick samples, the inverse of its square root is plotted against the applied heat external flux. The CHF is then identified as the x-axis intercept of the best-fit line through these data points ([7] Chapter 36). CHF can be estimated as Equation 2 indicates:

$$CHF \approx \sigma \cdot (T_{ign}^4 - T_0^4) \quad (2)$$

Where the  $\sigma$  is the Stefan-Boltzmann constant ( $56,7e-12 \text{ kW/m}^2 \cdot \text{K}^4$ ), and  $T_0$  is the ambient temperature. Despite the liquid state of the samples, which could induce convection currents due to temperature gradients within the layers, the thermal exposure originates from the topside. This results in a stratified configuration, with the hottest and least dense layers located at the top. Consequently, the potential influence of convection currents is expected to be minimal and a temperature gradient within the liquid is expected to prevail. Based on this assumption and the application of the Biot number (Bi), the samples analysed in this work are classified as thermally thick, according to Equation 3 [5]:

$$Bi = h \cdot L/k \quad (3)$$

Where  $h$  is the coefficient of the convective heat transfer coefficient ( $\text{W/m}^2 \cdot \text{K}$ ),  $L$  is the characteristic longitude (m) and  $k$  is the thermal conductivity ( $\text{W/m} \cdot \text{K}$ ). The Biot values for the samples ranged from 0,34 to 1,48 for heat fluxes of  $50 \text{ kW/m}^2$  and  $35 \text{ kW/m}^2$ , respectively.

The Thermal Response Parameter (TRP) reflects the resistance of a given material to ignition and fire propagation. The higher the TRP value, the longer it takes for the material to heat up and ignite. Next Equation 4 [7] defines the TRP:

$$TRP = \left( \frac{\pi}{4} \cdot k \cdot \rho \cdot c_p \right)^{0,5} (T_{ign} - T_0) \quad (4)$$

For thermal thick materials, the TRP, TTI and the thermal inertia are related in Equation 5:

$$t_{ign} = \left( TRP / \dot{q}'' \right)^2 \quad t_{ign} < t \quad (5)$$

Equations 2 to 4 enable the calculation of these parameters based on the obtained results. At the ignition instant, the Equation 5 becomes as Equation 6 [6], allowing estimating the TRP, although Thermal inertia ( $k\rho c_p$ ) is not available at this temperature:

$$t_{ign}^2 = TRP / \dot{q}_{ign}'' \quad (6)$$

Since the surface temperatures of the samples were obtained from thermocouple measurements during the lowest heat flux tests ( $T_{ign}$ ), the thermal inertia ( $k\rho c_p$ ) at the ignition moment could be

calculated. Notably, for edible oils, calculating thermal properties above frying temperatures (typically less than 200 °C) is rarely performed due to their primary application in cooking.

Three of the most consumed edible oils globally in 2022 (in million metric tons) [8] were analysed: soybean (60,24), rapeseed (28,85), and sunflower (20,87). The oils were pure (unblended) and unused, i.e., they had not been previously heated or used for cooking.

## 2. Experiments

Cone calorimeter testing was employed to assess the response of materials exposed to controlled radiant heat fluxes of 35 and 50 kW/m<sup>2</sup>. A FTT-Fire Testing Technology cone calorimeter was utilized for this purpose. Three replicate tests were conducted for each sample and heat flux combination to ensure the repeatability of the results. For each test, 100 ml (1 cm deep) of oil was poured onto the square sample holder without using a retainer frame for molten materials or a grid. At a heat flux of 35 kW/m<sup>2</sup>, the sample temperature was monitored at three depths: the upper layer, 2 mm depth, and 5 mm depth using three thermocouples positioned within the sample holder. For the 50 kW/m<sup>2</sup> heat flux, additional tests were conducted without a spark igniter to investigate the potential influence of the spark igniter and to assess any differences in behaviour between auto-ignition and pilot ignition.

## 3. Experimental results

Table 1 summarizes the TTI measured in the tests, the ignition temperature, the CHF, the TRP, Biot number and thermal inertia. While Figure 1 presents the best-fit curves plotted against the square root of the inverse of the TTI, Figure 2 shows the evolution of the temperatures at three different depths.

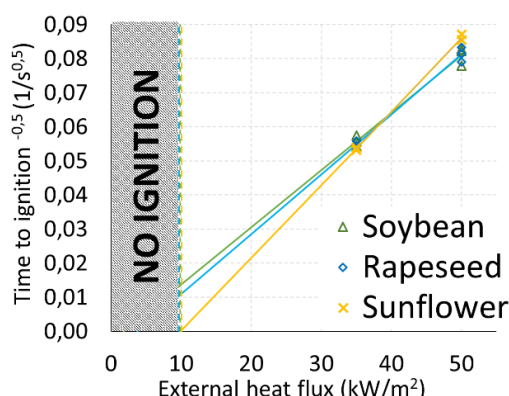


**Figure 1.** Square root of inverse of ignition vs external heat flux.

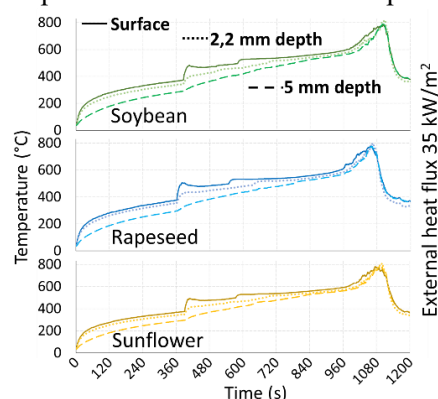


**Figure 2.** Temperatures measured at three different depths: surface, 2,2 mm and 5 mm.

**Table 1.** TTI (average), CHF, TRP, Biot number and thermal inertia.

Parameters	Soybean	Rapeseed	Sunflower
TTI at 35 kW/m <sup>2</sup> (s)	323	332	348
TTI at 50 kW/m <sup>2</sup> (s)	153	152	135
Surface temperature at TTI at 35 kW/m <sup>2</sup> (°C)	379	377	383
CHF (kW/m <sup>2</sup> )	9,8	9,7	10,0
TRP (kW·s <sup>0.5</sup> /m <sup>2</sup> )	176	176	187
Biot at 35 kW/m <sup>2</sup> (-)	1,41	1,48	1,45
Biot at 50 kW/m <sup>2</sup> (-)	0,34	0,36	0,35
Thermal inertia ( $k\rho c_p$ ) (kJ <sup>2</sup> /m <sup>4</sup> ·s·K <sup>2</sup> )	0,30	0,31	0,34

In both heat fluxes, the three oils exhibited very similar behaviour, with highly comparable ignition times and ignition temperatures. These values result in similar calculated critical heat fluxes and TRP values among the oils. The evolution of temperatures in Figure 2 exhibits similar heating trends for the oils. The recorded ignition temperatures (between 377 and 383 °C) were also similar, with no significant differences observed between the oils. While the differing heating rates of the liquid layers could

potentially induce convection currents, these currents are expected to be weak. This is because the thermal exposure originates from the top surface of the sample, resulting in a stratification with the hottest and least dense layers situated at the top. The use of different depths revealed a temperature gradient within the liquid. The smoke point, the temperature at which oil produces a continuous wisp of smoke, for soybean, rapeseed, and sunflower were 253 °C, 236 °C and 287 °C, respectively. Notably, these values are significantly lower than the corresponding ignition temperatures. Therefore, the appearance of smoke during cooking can be interpreted as a crucial early warning sign, indicating that the oil has reached a high temperature but remains below its ignition point.

One of the most important parameter provided by the cone calorimeter is the evolution of mass loss when the samples are exposed to an external heat flux. The specific mass loss rate (sMLR) variations observed during the tests are illustrated in Figure 3. In this Figure, circles, dots and cross are the values for the tests, while solid and dashed lines are the average values of the three tests at 35 kW/m<sup>2</sup> and 50 kW/m<sup>2</sup> respectively. The behaviour of the three oils exhibited high similarity. Notably, the time to ignition for all three oils ranged between 303 seconds and 345 seconds when the heat flux was 35 kW/m<sup>2</sup>, and between 132 and 165 seconds when the external heat flux was increased to 50 kW/m<sup>2</sup>. Increasing the external heat flux ( $\dot{q}_{ext}$ ) not only advanced the ignition time by approximately 56%, but also resulted in a greater increase in sMLR. The average mass loss rate increased from 12,78 g/s·m<sup>2</sup> at 35 kW/m<sup>2</sup> to 17,10 g/s·m<sup>2</sup> at 50 kW/m<sup>2</sup>. The triangular shape of the sMLR curves, lacking a plateau indicative of a constant mass loss rate, suggests that a steady-state burning rate was not achieved.

According to Equation 7, the burning rate per unit area ( $\dot{m}''$ ) is directly proportional to the incident heat flux ( $\dot{q}_{ext}$ ) and depends on the energy required to vaporize the material ( $L_v$ ):

$$\dot{m}'' = \dot{q}_{ext} / L_v \quad (7)$$

The energy required to vaporize the material ( $L_v$ ) can be determined using Equation 8, which describes the relationship between the mass loss rate, the energy released and the flame heat flux net from the flame [9]:

$$sMLR = \left(1/L_v\right) \cdot \dot{q}_{ext} + \left( Flame\ Heat\ Flux_{net} / L_v \right) \quad (8)$$

Where the slope of the best fit line (indicated as solid line) of the relation between the external heat flux ( $\dot{q}_{ext}$ ) and the average of sMLR of the tests as Figure 3 depicts. The term flame heat flux net refers to the heat flux from the flame minus the radiative heat flux losses from the sample surface ( $\epsilon\sigma T_{ign}^4$ ). In Table 2, the average values of the three tests for each type of oil are compiled, including sMLR, peak sMLR, and the heat of vaporization.

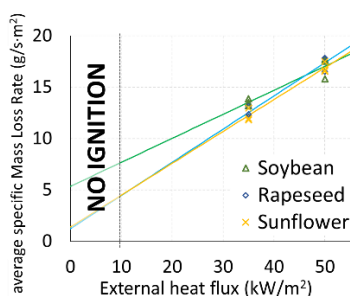


**Figure 3.** Average specific mass loss rate vs external heat flux.

The observed heats of vaporization for the edible oils ranged from 3,09 kJ/g to 4,31 kJ/g, whereas the sMLR peak values were between 21,02 g/s·m<sup>2</sup> and 21,85 g/s·m<sup>2</sup> at an external heat flux of 35 kW/m<sup>2</sup> and, at 50 kW/m<sup>2</sup>, the sMLR peaks ranged from 27,48 g/s·m<sup>2</sup> to 29,90 g/s·m<sup>2</sup>.

The HRR is the primary parameter used to characterize the burning behaviour of a material. Cone calorimetry, based on the principle of oxygen consumption, is a standard technique for measuring HRR, ISO 5660-1 [10]. Figure 5 presents the evolution of the HRR curves, which exhibit a very similar shape

**Table 2.** Average values for sMLR, peak mMLR and  $L_v$ .

Parameters	Soybean	Rapeseed	Sunflower
Av sMLR at 35 kW/m <sup>2</sup> (g/s·m <sup>2</sup> )	13,54	12,54	12,25
Peak MLR at 35 kW/m <sup>2</sup> (g/s·m <sup>2</sup> )	21,82	21,02	21,65
Av sMLR at 50 kW/m <sup>2</sup> (g/s·m <sup>2</sup> )	17,01	17,39	16,90
Peak sMLR at 50 kW/m <sup>2</sup> (g/s·m <sup>2</sup> )	27,48	29,90	27,96
Heat of vaporization ( $L_v$ ) (kJ/g)	4,31	3,09	3,22

to the previously observed sMLR curves (Figure 4). Since the energy production per unit area is related mass loss ( $\dot{m}''$ ) as indicated in Equation 9, the effective heat of combustion (EHC)( $\Delta H_{comb}$ ) can be obtained.

$$\dot{Q}'' = \dot{m}'' \cdot \Delta H_{comb} \quad (9)$$

Similar to the MLR curves, the HRR curves displayed comparable behaviour for all oils. As the external heat flux increased, the mass loss rate also increased, with the HRR reflecting this trend. Consequently, the average and peak HRR values were significantly higher for the 50 kW/m<sup>2</sup> external heat flux compared to the lower flux. For example, the peak HRR (average of 3 tests) for soybean oil at 35 kW/m<sup>2</sup> was 691 kW/m<sup>2</sup>, whereas it reached 965 kW/m<sup>2</sup> at 50 kW/m<sup>2</sup>.

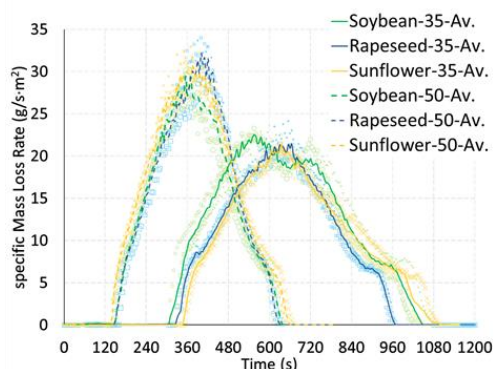


**Figure 4.** Evolution of the sMLR curves.

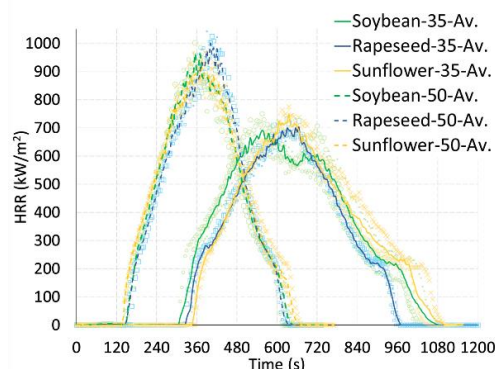


**Figure 5.** Evolution of the HRR curves.

Since in all tests was employed identical initial amount of oil and a near-complete mass loss was observed, the THR, calculated as the integral of the HRR over the test duration, showed similar values for all samples. The EHC obtained and other parameters, including the total energy released (THR), and the peak and average HRR values, are presented in Table 3.

**Table 3.** Average values obtained from the three tests: HRR, EHC and THR.

Properties	35 kW/m <sup>2</sup>			50 kW/m <sup>2</sup>		
	Soybean	Rapeseed	Sunflower	Soybean	Rapeseed	Sunflower
HRR peak (kW/m <sup>2</sup> )	691	702	748	965	1000	913
HRR average (kW/m <sup>2</sup> )	415	412	429	557	541	506
Peak EHC (MJ/kg)	34,7	37,3	37,1	37,6	36,1	34,5
Av EHC (during flaming period)(MJ/kg)	28,8	32,0	33,0	32,7	31,1	29,8
Total Heat Release (MJ/m <sup>2</sup> )	267,7	215,9	267,0	259,7	254,3	262,7

The final aspect investigated in this study was the influence of the spark igniter employed in cone calorimetric tests. While the previously presented results were obtained using a spark igniter, real-world kitchen fires typically do not involve external ignition sources. Instead, kitchen fires often is produced by raising the temperature of the whole volume of gas released up to it ignites. This term is referred as auto ignition temperature (AIT), i.e. the spontaneous ignition due to self-heating and without an external ignition source. No significant differences were observed in the TTI, and the resulting MLR curves were similar to those obtained with the spark igniter. These findings suggest the applicability of our results using the spark igniter to scenarios lacking an external ignition source.

#### 4. Discussion and conclusions

The obtained information provides valuable insights into their thermal behaviour, explaining why they pose a significant fire risk at high temperatures. A key characteristic of edible oils is their relatively high flash point. The flash point refers to the temperature at which a liquid releases sufficient volatile products to form a flammable mixture with air that can ignite momentarily upon exposure to a spark or flame, but cannot sustain combustion independently [5]. Consequently, the values of the temperatures measured at the pilot ignition ranged between 377÷383 °C and agree with values reported in literature

[11, 12]. Interestingly, edible oils exhibit significantly higher flash points compared to industry oils. For instance, diesel and kerosene have flash point of  $50\div 77$  °C [12] and 47,8 °C [13] respectively, whereas the flash point for edible oils typically exceeds 300°C [12]. This substantial difference highlights a unique feature of edible oils: while a larger temperature increase is necessary for ignition, this value may well be reached in normal cooking operational conditions. Other parameters found such  $L_v$  and  $\Delta H_{comb}$  for the edible oils were similar with the observed for other liquid combustibles. For instance, the  $\Delta H_g$  for acetone is 5,01 kJ/g and 8,37 kJ/g for ethanol [7]. As for  $\Delta H_{comb}$ , which provides a quantitative value for the amount of energy a material releases per unit mass when it burns completely, the obtained values revealed values consistent with previous literature, e.g. 39,0 MJ/kg for soybean [11], 36,6÷37,7 MJ/kg for rapeseed and 39,28 MJ/kg for sunflower [12]. These findings align with the EHC values obtained for other common cooking oils, such as olive (39,6 MJ/kg) and corn (39,4 MJ/kg) [13]. And yet, these values were slightly lower than those for industrial oils such as kerosene (43.2 MJ/kg [7]) and diesel (41.36 MJ/kg [14]). This particular behaviour of edible oils helps to make initial ignition more difficult, it also presents a potential hazard once a fire is triggered. The most common cause of cooking fires is unattended cooking, leading to a significant increase in oil temperature up the autoignition point. This scenario translates to a situation where the oil temperature exceeds significantly its flash point, leading to fires exhibiting the characteristics previously highlighted previously discussed in the introduction.

## 5. Acknowledgments

The authors express their deepest gratitude to “BSH Electrodomésticos España S.A. – Centro de Desarrollo de Gas”; Nuclear Safety Council “Metodologías avanzadas de análisis y simulación de escenarios de incendios en centrales nucleares” and NEXT (Sistema inteligente de apoyo a la prevención y gestión de emergencias industriales en Cantabria (2023/TCN/004 - Financiado por el Gobierno de Cantabria/FEDER, UE).

## 6. References

- [1] Ahrens M and Maheshwari R. 2021 Home structure fires. *NFPA. Fire Analysis and Research*.
- [2] Ahrens M. 2021. *NFPA. Fire Analysis and Research*.
- [3] Hamins A, Kim SC and Madrzykowski D. 2018 Characterization of stovetop cooking oil fires. *J. Fire Sci*, **36**(3), pp. 224-239.
- [4] Xu X, Wang P, Yu N and Zhu H. 2019. Experimental Study on Kitchen Fire Accidents in Different Scenarios. In *9th Int. Conference on Fire Sci. and Fire Protection Engineering*, pp 1-6. IEEE.
- [5] Babrauskas V. 2003 Ignition handbook. Fire science publishers/society of fire protection engineers.
- [6] Quintiere JG. 2006. A theoretical basis for flammability properties. *Fire Mater*, **30**(3), pp 175-214.
- [7] Hurley MJ, Gottuk DT, Hall JR, Harada K, Kuligowski ED, Puchovsky M, Torero JL, Watts JM and Wieczorek C. 2016. *SFPE Handbook of Fire Protection Engineering*; Springer.
- [8] Consumption of vegetable oils worldwide from 2013/14 to 2021/22, by oil type. 2022. <https://www.statista.com/statistics/263937/vegetable-oils-global-consumption/>. Last access: January 2024.
- [9] Luche J, Rogaume T, Richard F and Guillaume E. 2011. Characterization of thermal properties and analysis of combustion behavior of PMMA in a cone calorimeter. *Fire Saf. J*, **46**(7), pp 451-461.
- [10] ISO 5660-1:2015. Reaction-to-fire tests — Heat release, smoke production and mass loss rate — Part 1: Heat release rate (cone calorimeter method) and smoke production rate (dynamic measurement). 2015. *ISO – International Standard Organization*.
- [11] Shahidi F. 2005. *Bailey's Industrial Oil and Fat Products, Industrial and Nonedible Products from Oils and Fats*. **6**. *John Wiley & Sons*.
- [12] Bockisch M. 1998. *Fats and oils handbook. Academic Press and AOCS Press*. Elsevier.
- [13] Gravalos I, Gialamas T, Koutsofitis Z, Kateris D, Tsiropoulos Z, Xyradakis P and Georgiades, A. Energetic study on animal fats and vegetable oils using combustion bomb calorimeter. 2008. *Journal of Agricultural Machinery Science*, **4**(1), 69-74.
- [14] Andrade RD, Faria EA, Silva AM, Araujo WC, Jaime GC, Costa KP, and Prado AG. 2011. Heat of combustion of biofuels mixed with fossil diesel oil. *J. Therm. Anal. Calorim.*, **106**(2), 469-474.